Egypt. J. Chem. **Vol. 67**, No. 5 pp. 413 - 423 (2024)

Egyptian Journal of Chemistry

http://ejchem.journals.ekb.eg/

Utilized The (Maleic) Acid Anhydride Grafted Cellulose To Sorption Of Cu(II), Mn(II), Cd(II), Fe(III) and Pb(II) In Water Sample

Mahmoud A. Hammad [a], Shimaa G. Hussien [a], Fathy A. El-Saied [a], Mustafa M. Kamel [b], Saeyda A. Abouel-Enein [a*]

[a*] *Department of Chemistry, Faculty of Science, Menoufia University, Shebin El Kom, Egypt*

[b] *El-Nasr Company for Intermediate Chemicals, Giza, Egypt*

Abstract

This work investigated the ability of maleic acid anhydride grafted cellulose functionalized with thiourea (Cell-THU) to adsorb Cu (II), Mn (II), Cd (II), Fe (III) and Pb (II) ions from aqueous solution. Using a variety of conditions including adsorbent dose, pH, contact time, metal cations concentration and temperature at 500 rpm, the process of adsorption for this produced adsorbent to remove the analyzed metal cations was examined in a batch technique. The mechanism of adsorption process is declared by applying different kinetics and isotherm models. Maximum adsorption capacities for Cu (II), Mn (II), Cd (II), Fe (III) and Pb (II) were 29.85, 25.91, 31.84, 26.18, and 33.22 mg/g, respectively at pH=7, adsorbent dose=0.3 g, contact time=90 min. and initial metal cation concentration (3 mg/L) at room temperature (25°C) . With that maximal adsorption capacity, the Langmuir isotherm produces the best match to the equilibrium data. Data analysis using kinetics revealed that the adsorption related to pseudo 2nd order model. It was observed that Cell-THU performs really well for eliminating toxic metal ions.

Keywords: Adsorption; maleic anhydride; heavy metal ions; kinetic; adsorption isotherm.

1. Introduction

Water contamination, particularly pesticide and heavy metal pollution, has become one of the causes which exhibit numerous effects on different organisms due to their excessive release from various effluents [1, 2]. Due to heavy metals accumulation in biological systems and consumption of food contaminated with them causes risk to human's health [3-5]. These metals generate severe toxicity, harmful effects on living things and for environment due to their aggregation in the food chain since they are released into water sources in large quantities [6]. Moreover, because heavy metals are not degraded by bacteria after being secreted into the atmosphere, they can have hazardous effects on the environment and later on biological systems [7]. The World Health Organization (WHO) put limits on the quantities of heavy metals that can be found in drinking water as their negative effects to all living things (including humans, animals, and plants) [8].

Hence, several methods have been used including physical, chemical and biological ones to eliminate heavy metals from wastewater [9]. Other techniques also involve ion exchange, membrane filtration, biological systems, adsorption techniques, oxidation, precipitation and solvent extraction using electrolytic procedures. In adsorption techniques it is preferred to use natural polymer adsorbents because they are renewable, less hazardous, adaptable to change, biodegradable and inexpensive [10]. Natural-based polymers as chelating adsorbents may be used due to the biopolymer-based adsorbents' functional groups improve the effectiveness of elimination of heavy metals from samples of water by forming complexes with chelating metal ions [9].

The world's most common, sustainable and naturally occurring polymer is cellulose which is a long-chained linear polysaccharide made up of β-D-glucopyranose units connected through -1,4-glycosidic linkages [11]. Two hydroxyl groups and one methylol of the cellulose molecule serve as functional groups in one repeating unit [12]. Due to the strong bonds of hydrogen between the chains of

* Corresponding author E-mail: dr.saeyda_elenein@yahoo.com

Receive Date: 14 August 2023, Revise Date: 20 October 2023, Accept Date: 31 October 2023

DOI: 10.21608/EJCHEM.2023.224235.8435

cellulose, cellulose is extremely crystalline and typically insoluble in common solvents even in water.

The modification methods include polymer-polymer blending, derivative formation, crosslinking and grafting [13]. Graft copolymerization is a popular technique for modifying the surfaces of polymers [11]. and it is an essential method for improving the chemical or physical properties of polymers. During grafting, the side chains are covalently joined to the backbone of the substrate or primary polymer to produce a copolymer with a branched structure. Resulted graft copolymers acquire additional qualities including increased elasticity, hydrophilicity or hydrophobicity, ion-exchange capacities, thermosensitivity, pH sensitivity, resistance to heat and microbial activity, etc [11].

This paper concerned to modify the structure of cellulose by using maleic anhydride then the grafted copolymer was reacted with thiourea. The resulted adsorbent used for removing Cu (II), Mn (II), Cd (II), Fe (III) and Pb (II) cations from contaminated water. This adsorption process was optimized by investigating adsorbent dose, pH, contact time, temperature and initial metal cation concentration .To simulate the adsorption characterization, models of Freundlich and Langmuir isotherm were studied. The kinetic analysis was also studied.

2. Experimental

2.1. Instruments and chemicals

Cellulose (Cell), maleic anhydride, ferrous sulphate (FeSO4.7H2O), hydrogen peroxide (H2O2), acetic acid (CH3COOH) and thiourea. Analytical-grade chemicals were employed to prepare the metal ion aqueous solutions used in the current experiment. Separate stock solutions of 1000 mg metal ion/L of Cu(II), Mn(II), Cd(II), Fe(III) and Pb(II) were made from CuSO4.5H2O, MnCl2.4H2O, FeCl3.6H2O, CdCl2.H2O, and Pb(NO3)2, respectively. A number of diluted solutions were made using these stock solutions. 1.0 M of HCl solution and 1.0 M of NaOH solution were employed to modify the pH of solutions with a pH range of 1 to 9. Using a pH meter (WTW-inolab in Germany), the solutions' pH values that were produced was identified. The residual concentrations were determined using a Flame Atomic Absorption Spectrophotometer (FAAS) (Perkin Elmer 503) and a calibration curve produced using standard metal ion solutions. The KBr pellet technique on a Nicolet FT-IR spectrophotometer between 4000 and 400 cm-1 was used to indicate the most functional groups. Utilizing a Shimadzu DT/TG-50 and a nitrogen environment with heating rate of 10 °C/min, thermogravimetric analysis (TGA) was carried out. Data from X-ray powder diffraction experiments (XRD) were gathered using a Philips PW 3710/31 X-ray generator and an automatic sample changer (scintillation counter, Ni-filter at 40 Kv and 30 mA and Cu-target tube).Using a scanning electron microscope (SEM) (JSM-5300, JEOL Ltd.), surface size was determined. In order to increase conductivity, gold was sputtered onto the SEM specimens using a JEOL-JFC-1100E coating process.

2.2. Adsorbent preparation

2.2.1. Grafting of cellulose

50 mL of distilled water were used to suspend a sample of 1 g of cellulose (Cell) for one hour, then 1 g of maleic anhydride was added. After that, 1 mL of H_2O_2 was poured while stirring continuously then 0.4 g ferrous sulphate was added. The final step, 0.7 mL of concentrated CH_3COOH was added. This process lasted for 3 hours under reflux at 80°C then filtered off, washed multiple times by de-ionized water until pH of filtrate reaches 7 then dried over anhydrous $CaCl_2$ in a vacuum desiccator.

2.2.2. Grafted cellulose's functionalization

Thiourea was added to the grafted cellulose prepared from the previous step according to: 1 g of grafted cellulose was added to 4 g of thiourea dissolved in 15 ml ethyl alcohol and 2 mL DMF. The mixture lasted for 36 h. The resulted product was filtered off, washed many times by de-ionized water and dried over anhydrous $CaCl_2$ in a vacuum desiccator. The immobilization of thiourea onto grafted cellulose is clarified in scheme 1.

2.3. Batch adsorption study

The pH impact was studied after adjusting pH of solutions from 1 to 9 using 1.0 M of HCl and 1.0 M NaOH. Also the impact of contact time in the range of (10-90 min) was illustrated. The effect of initial metal ion concentrations and adsorbent dosage was revealed in the range of 2–20 ppm and (0.1 – 0.5 g), respectively. Also the effect of temperature was examined. The solutions were filtered off by 0.45 μm filter membrane. Utilizing an atomic absorption spectrometer, remaining concentrations were measured. Using the equations S1 and S2 in the supplementary materials, the adsorption capacity and the removal percentage were calculated.

Scheme 1. Thiourea schematic immobilization onto grafted cellulose

Adsorption kinetics: The kinetics of adsorption onto grafted cellulose are modeled using pseudo-1st-order (Eq. S3) and pseudo-2nd-order (Eq. S4) equations [14-17].

Adsorption isotherms: The study of Adsorption isotherm was done using Langmuir and Freundlich isotherm (Eq. (S5) and (S6)) [18-20].

3. Results and Discussion

3.1. Adsorbent Characterization

Elemental analysis

Following the data in Table (1), modified cellulose has a lower percentage of carbon and hydrogen than cellulose. The analysis also revealed that the modified product includes 20.32% sulphur and 21.74% nitrogen. This emphasizes thiourea immobilized on grafted cellulose.

Table 1. Elemental analyses of the cellulose and modified cellulose

Sample	C%	H%	N%	S%
Cellulose	69.17	6.84	-	-
Cell-THU	60.95	5.36	21.74	20.32

Infrared spectral studies

The IR spectra of cellulose, grafted cellulose and thiourea grafted cellulose (Cell-THU) were collected in (Figure 1a-c). The cellulose spectra showed a broad band at 3347 cm^{-1}, that was related to stretching vibration of the OH groups. The spectral bands at 1060 cm^{-1} and 2901 cm^{-1} were ascribed to υ(–C–O–C) pyranose ring and υ(–C–H), respectively [21]. Other additional bands appeared in the region of 1430-1265 cm^{-1} were due to (O-H) bending and (C-OH) stretching vibrations [22]. However, the observed band at 1642 cm^{-1} was assigned to the deformation vibration of the hydroxyl groups δ (OH) [22]. Other bands within the region below 1000 cm^{-1} were due to alcohol groups' absorption [23]. The spectrum of grafted cellulose declared a new vibration bands at 956 cm^{-1}, 853 cm^{-1} and 809 cm^{-1} that characterized to (–O–) ring of maleic anhydride moieties grafted onto cellulose. However, the novel spectral bands at 1701, 1743, 1795, 1836 and 1869 cm^{-1} were attributed to υ(C=O) of cellulose ring rupturing [24, 25]. and maleic anhydride, respectively. It is observed that there was a differ in the bands shape in remote region which confirmed υ(C-C=O). The grafting process was confirmed by all of these detected bands [26]. The IR spectrum of thio aminated grafted cellulose showed peaks at 3449, 3412; 1521 and 965 cm^{-1} that could be connected to υ, δ and γ of NH_2 and NH groups [27]. A new band in the spectrum revealed at 732 cm^{-1} not observed on starting material pointed to υ(C=S) [28]. The above observations state the formation of Cell-THU. However the spectrum of Cell-THU after adsorption of the metal ions delineates in Figure 1-d. The spectrum exhibits shifts in the bands at (3449, 3412, 1743, 732 cm^{-1}), denoting to the uptake of the metal ion takes place chemically via binding the metal ion with the activated functional groups NH_2, N-H, C=O, and C=S.

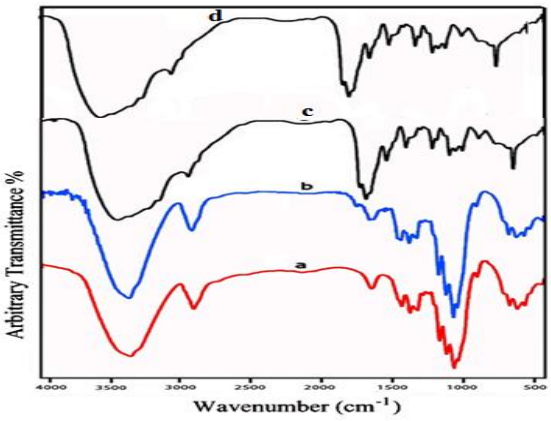

Fig. 1. IR spectrum of cellulose (a), grafted cellulose (b), Cell-THU (c) and Cell-THU after adsorption (d)

SEM micrograph

The SEM is a method that describes the constituent and surface topography of the material. To examine surface morphology of (Cell-THU) a SEM micrograph was done. SEM image (Figure S1) reveals that the product's surface has holes and pore spaces of irregular shapes that are suitable for adsorbing metal ions from liquids.

X-ray diffraction analysis

This analysis was employed to inform the crystal system type and lattice parameters of the materials. The cellulose and thio aminated cellulose (Cell-THU) powder XRD patterns were shown in (Figure S2 and S3). Cellulose XRD pattern had three peaks at 2θ = 15.34º, 22.33º and 35.11º, related to cellulose crystal morphology, while XRD pattern of Cell-THU illustrated that the material is much more crystalline than cellulose and declared new peaks at 2θ =9.85º, 15.17º, 16.87º and18.10º.The powder XRD patterns of the cellulose was completely different from that of Cell-THU, implying the functionalization on the cellulose surface was achieved successfully.

Thermal analysis

Modification of cellulose was also predicted by thermal analysis. The cellulose and (Cell-THU) thermogram patterns outlined in Figure (S4). The cellulose had a weight loss of 10.87% due to dehydration in the range of 28-290°C then pyrolysis comes next at 290°C, while (Cell-THU) demonstrated a weight loss of 22.79% in the range of 25-188°C which has been related to the elimination of water molecules. After that cellulose and Cell-THU started decomposition at 290°C and 188ºC, respectively. The pyrolysis of cellulose was carried out by two separate steps. A large DTG peak was seen at Tmax = 334°C during the first pyrolysis, which was conducted at a constrained temperature range of 290-370°C with a significant weight loss of 69.16%. This demonstrates that cellulose breakdown was both speedy and gradual. A medium-broad DTG peak at Tmax=306 degrees Celsius served as an indicator for the initial pyrolysis of Cell-THU, which occurred throughout a wide temperature range from 188 to 580 degrees Celsius and resulted in a weight loss of 29%. This indicates that cellulose had a greater rate of degradation than Cell-THU and was more stable than its modified version. It might be caused by the graft polymerization process rupturing certain cellulose rings [21].

3.2. Analysis of batch adsorption data

Impact of pH

Figure 2 represents the percentages of removal for Cu(II), Mn(II), Cd(II), Fe(III) and Pb(II) cations onto prepared adsorbent (Cell-THU). With increasing pH, the removal of all metal ions increases where the maximum values of removal of Cu(II), Fe(III) and Pb(II) was 78%, 97% and 93% at (pH=6) , respectively, however in case of Mn(II) and Cd(II) reported maximum value 80% and 91% at (pH=7), respectively. The main causes are the functional groups' extensive protonation which results in electrostatic repulsions between the heavy metal ions and the protonated groups [29]. This is normally the situation in environments with lower pH levels and high proton availability. Another phenomenon that could exist in situations with lower pH levels is the ineffective adsorption caused by the competing adsorption of hydronium ions (H3O+) with the positively charged metal species. However, at higher pH levels may lead to the formation of metal ion hydroxylated complexes, which would inhibit the action by restricting the surface moieties [30].

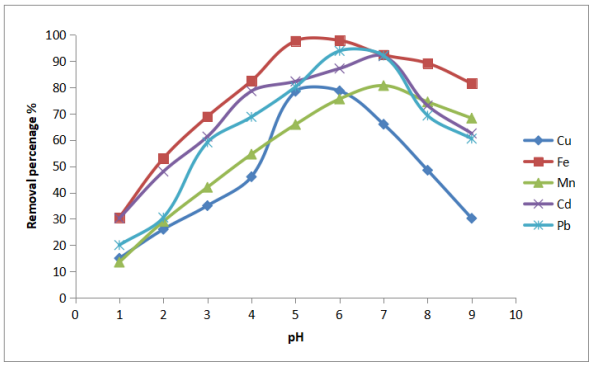

Fig. 2. Impact of pH on metal cations removal

Impact of adsorbent dosage

Figure 3 shows removal percentages for studying metal ions onto adsorbent as a function of adsorbent dosages. The results show that removing increases by increasing dosage reaching its maximum at 0.3gm of adsorbent. This is because the adsorbent's surface area has increased, increasing the amount of active surfaces which are readily accessible for a given volume of liquid, increasing the overall amount of metal ion removal [31,32].

Impact of contact time

Figure 4 illustrates the relationship between the percentages of examined metal ions removed from produced adsorbents and different times. The data recorded removal percentage of 53 %, 50 %, 56%, 43% and 45 % for Cu(II), Mn(II), Cd(II), Fe(III) and Pb(II) cations, respectively during the first

20 min. Within 90 minutes, all metal ions had been removed to 100% of their original percentage. Because there are a lot of empty surface sites available during the early stages of sorption, the percentage of metal ion removal that increases with contact time is explained. After some time, saturation makes it challenging to fill the remaining open surface sites [33].

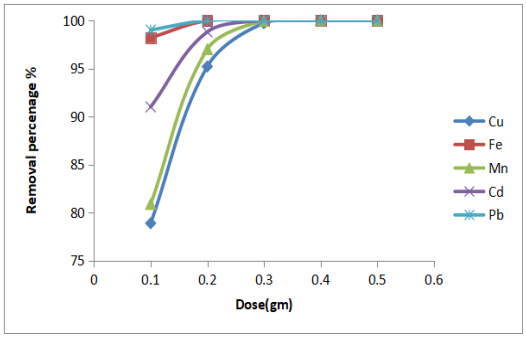

Fig.3. Impact of adsorbent dosage on metal cations removal

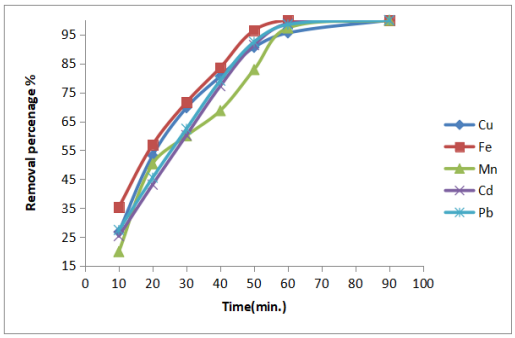

Fig. 4. Impact of contact time on metal cation removal

Impact of heavy metal concentration

The obtained data are diagramed in Figures 5. It was discovered that at low concentrations there are less accessible metal ions for adsorption which results in a better adsorption efficiency. As it increases, the number of ions available for the adsorption increases, which results in a lower adsorption rate. However, the amount of saturated sites can still adsorb additional ions up to a specific concentration. This results in a decrease in adsorption efficiency for a given amount of accessible adsorbent [34]. The higher adsorption value of all metal ions is 100% at initial concentration (C_o=3 mg/L).

Impact of temperature

Figure 6 indicates the influence of temperature on the efficiency of removal for different metal ions.

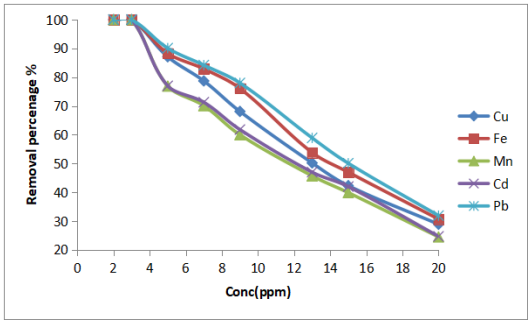

Fig. 5. Impact of initial concentration on metal cations removal.

The data reports the sorption efficiency decreased from 30 to 60 oC. According to thermodynamics: for an endothermic process, the adsorption capacity increases as the temperature rises and decreases for an exothermic process [35]. The fact that the removal effectiveness decreased as the temperature increased indicates that the process of adsorption is exothermic. Higher temperatures reduce the electrostatic interactions which linked the metal ions with the adsorbent, increasing the metal ions' mobility and causing them to separate from the adsorbent which results in lower adsorption [36].

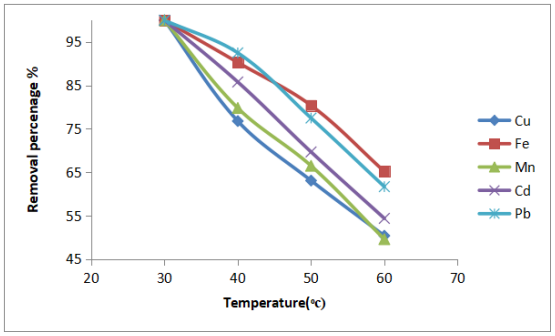

Fig.6. Impact of temperature on removal percentage of metal cations

Adsorption kinetics:

Studying of adsorption kinetics is significant because it gives evidence of the adsorption mechanism needed for the process' effectiveness [37, 38]. Adsorption kinetics was investigated at different contact time and data was analyzed to know which model is better to explain adsorption of Cu(II), Mn(II), Fe(III), Cd(II) and Pb(II) ions. Figure 7 and 8 correspond to pseudo-1st-order model and pseudo-2nd-order model for the ions, respectively.

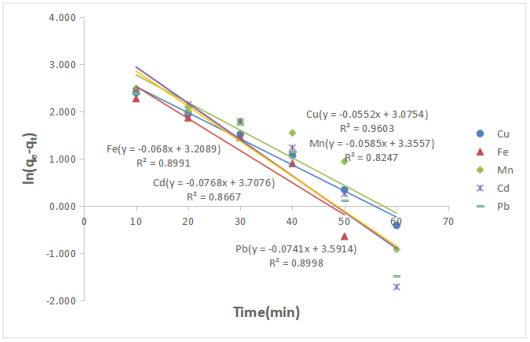

Fig. 7. Model of Pseudo-1st-order

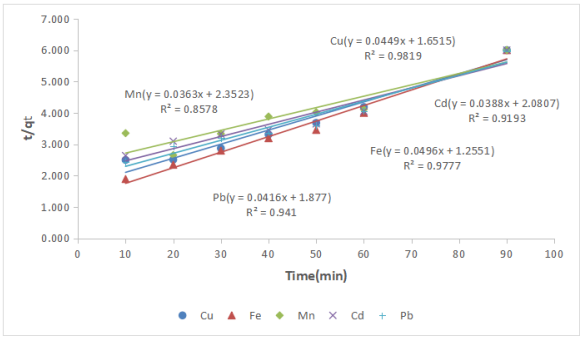

Fig. 8. Model of Pseudo-2nd-order

Table 2. Calculated kinetic models parameters

	Parameters	Cu^{2+}	Mn^{2+}	Fe^{3+}	Cd^{2+}	Pb^{2+}
Pseudo-1st-order	**K_1 (min^{-1})**	0.0552	0.0585	0.068	0.0768	00.0741
	q_e cal.(mg/g)	21.658	28.665	24.751	40.755	36.284
	R^2	0.9603	0.8247	0.8991	0.8667	0.8998
Pseudo-2nd-order	**K_2(g/mg min)**	0.00122	0.00056	0.00196	0.00072	0.00092
	q_e cal.(mg/g)	22.271	27.548	20.161	25.773	24.038
	R^2	0.9819	0.8578	0.9777	0.9193	0.941
Experimental	**q_e Exp.(mg/g)**	15	15	15	15	15

This data shows that the pseudo-2nd-order model produces more straight lines than the pseudo-1st-order model due to its greater correlation coefficient R2 and qe values are closer to the experimental values. This demonstrates that chemisorption is the major process which depending on sharing electrons between the adsorbate and the surface of the adsorbent. Chemisorption is usually limited to a single layer of molecules on the adsorbent's surface [39].

Adsorption isotherms:

The mathematical model known as the adsorption isotherm describes how adsorbate species behave in both liquid and solid phases [40, 41]. At constant temperature and various ion concentrations, the adsorption isotherm was studied. Freundlich and Langmuir isotherm models were used to analyze the equilibrium results for the adsorption of cations onto thio aminated cellulose (Cell-THU).

Only a single adsorption monolayer exists on an adsorbent in Langmuir isotherm models, which is based on surface homogeneity. This monolayer forms as a result of how the metal ions are distributed in equilibrium between the solid and liquid phases. There is no further adsorption when the adsorbate single layer forms on the adsorbent outer surface [42].

By plotting C_e/q_e vs C_e, Figure 9 reveals Langmuir models for the ions. The slope was used to compute the monolayer adsorption capacity q_{max} and the intercept was used to calculate K_L.

The adsorption on heterogeneous surfaces is best described using Freundlich isotherm models Figure 10, which are entirely empirical.

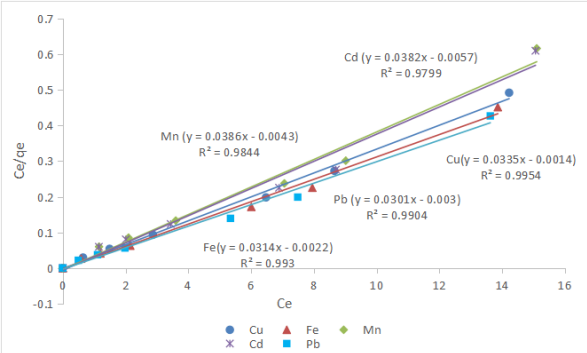

Fig. 9. Langmuir isotherm model

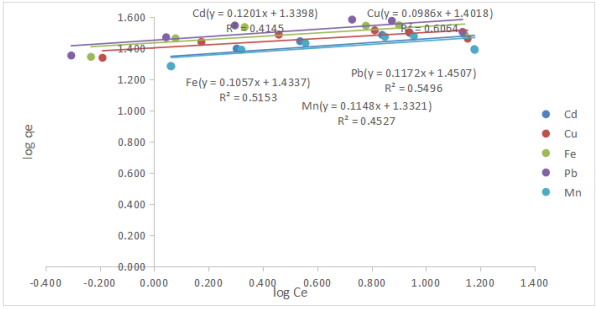

Fig. 10. Freundlich isotherm model

Table 3. Calculated isotherm parameters

	Parameters	Cu^{2+}	Mn^{2+}	Fe^{3+}	Cd^{2+}	Pb^{2+}
Langmuir	**K_L (L/mg)**	23.92	8.97	14.27	6.70	10.03
	q_{max} mg/g)	29.85	25.91	31.84	26.18	33.22
	R_L	0.002	0.005	0.003	0.007	0.004
	R^2	0.9954	0.9844	0.993	0.9799	0.9904
Freundlich	**K_F (L/g)**	25.22	21.48	27.14	21.86	28.22
	1/n	0.0986	0.1148	0.1057	0.1201	0.1172
	R^2	0.6064	0.4527	0.5153	0.4145	0.5496

According to the data, the Langmuir model predicts favorability as a result of RL which is greater than zero and less than unity. The Freundlish model predicts favorability as a result of 1\n which is greater than 0.1 and less than unity. However, because the R2 value of the model of Langmuir is greater than of the Freundlish model, so the process of the tested metal ions go along with the Langmuir isotherm model [43, 44].

3.3. Application to real underground water:

Underground water samples from the El-Meridian Hotel in El-Haram, Giza, Egypt, were taken in order to test the treatment process used to remove Cu (II), Mn (II), Cd (II), Fe (III) and Pb (II) ions from synthetic water. Membrane filter of 0.45µm was used to filter the sample. A flame atomic absorption spectrophotometer was used to measure the metal concentration in the water sample.

According to batch experimental results of removal of Cu(II), Mn(II), Cd(II), Fe(III) and Pb(II) ions from synthetic water, the optimum treatment conditions were pH = 7, dose = 0.3gm and time = 90 min.

In the experiment, 50 mL of water sample and 0.3 g of Cell-THU were combined. The mixture was lasted for 90 min at 500 rpm, pH 7 and (25 °C). Using 0.45µm membrane filter paper, suspensions were filtered and maintained for metal analysis.

The treatment data (Table 4) declared that the removal percentages were found to be 84-100%.

According to this, the researched adsorbent can be used to treat real samples due to its high efficiency and fast kinetics.

Table 4. Removal of Cu(II), Mn(II), Cd(II), Fe(III) and Pb(II) ions from underground water by Cell-Thiourea (Cell-THU)

Metal ions	Concentration (mg/L)		Removal percentage
	Before treatment	After treatment	
Cu(II)	3.0012	-	100%
Mn(II)	3.1121	-	100%
Fe(III)	7.2001	0.144	98%
Cd(II)	2.0213	-	100%
Pb(II)	3.6143	-	100%
Ni(II)	3.0145	0.434	85%
Cr(VI)	4.8811	0.7842	84%

Table 5. Comparison between the performance of maleic acid anhydride grafted cellulose functionalized with thiourea (Cell-THU) and other adsorbents reported in literature [45-50]

Adsorbents	Metal ions	Removal percentage %	Ref.
Grafted TEMPO-oxidized cellulose nanofiber embedded with modified magnetite	**Pb (II)**	**80%**	**[45]**
[a*]Cell-g-AASO$_3$H-co-AAc cross-linked graft copolymer	**Ni(II), Cu(II)**	**72%, 67%**	**[46]**
[b*]Cell-g-AASO$_3$H-co-AN	**Pb (II)**	**62%**	**[47]**
[c*]Cell-g-AASO$_3$H	**Pb (II)**	**59%**	**[47]**
Pristine cellulose nanocrystalline (CNC)	**Cd(II)**	**70%**	**[48]**
maleic anhydride functionalized cellulose nanocrystalline (MA-CNC)	**Cd(II)**	**90%**	**[48]**
[d*]CMC/SSS gels	**Cr(III), Pb(II), Mn (II), Fe (III)**	**68%, 41%, 35%, 33%**	**[49]**
Cellulose-graft-polyacrylic acid (cellulose-g pAA	**Pb(II), Cu(II), Cd(II)**	**94%, 65%, 26%**	**[50]**
Cellulose-g-p(AA–NMBA)	**Pb(II), Cu(II), Cd(II)**	**90%, 66%, 39%**	**[50]**
cellulose-g-p(AA–AASO3H	**Pb(II), Cu(II), Cd(II)**	**6%, 8%, 7%**	**[50]**
maleic acid anhydride grafted cellulose functionalized with thiourea (Cell-THU)	**Cu (II), Mn (II), Cd (II), Fe (III), Pb (II)**	**96%, 95%, 98%, 100%, 99%**	**This work**

*a: Cellulose grafted with 2-acrylamido-2-methylpropane sulfonic acid (AASO$_3$H) and acrylic acid in the presence of N,N'-methylene bisacrylamide cross-linker, *b: Cellulose grafted with 2-acrylamido-2-methylpropane sulfonic acid (AASO$_3$H), *c: Cellulose grafted with 2-acrylamido-2-methylpropane sulfonic acid (AASO$_3$H) and binary comonomer acrylonitrile (AN), *d: Sodium Carboxymethyl Cellulose (CMC-Na)/Sodium Styrene Sulfonate (SSS) hydrogels with grafted and crosslinked polymeric networks

Conclusion

maleic acid anhydride grafted cellulose functionalized with thiourea (Cell-THU) showed high efficiency for removal of Cu (II), Mn (II), Cd (II), Fe (III) and Pb (II) ions from aqueous solution. Maximum adsorption capacities for Cu (II), Mn (II), Cd (II), Fe (III) and Pb (II) were 29.85, 25.91, 31.84, 26.18, and 33.22 mg/g, respectively at pH=7, adsorbent dose=0.3 gm, contact time=90 min. and initial metal cation concentration (3 mg/L) at room temperature (25°C) . Langmuir isotherm produces the best match to the equilibrium data. Data analysis using kinetics revealed that the adsorption related to pseudo 2nd order model. The application data declared that the removal percentages were found to be 84-100%.

According to this, the Cell-THU can be used for eliminating toxic metal ions from real samples due to its high efficiency and fast kinetics.

Conflict of interest

The recommended reviewers and the authors do not have any conflict of interest.

References

1. Jawed A., Saxena V., Pandey L.M.; Engineered nanomaterials and their surface functionalization for the removal of heavy metals: a review, J. Water Process Eng., 33, 101009-101028 (2020).
2. Singh S., Kumar V., Chauhan A.; Toxicity, degradation and analysis of the herbicide a trazine, Environ. Chem. Lett., 16, 211–237 (2018).
3. Djahed B., Taghavi M., Farzadkia M., Norzaee S., Miri M.; Stochastic exposure and health risk assessment of rice contamination to the heavy metals in the market of Iranshahr, Iran. Food Chem. Toxicol., 115, 405–412 (2018).
4. Fakhri Y., Saha N., Miri A., Baghaei M., Roomiani L., Ghaderpoori M., Taghavi M., Keramati H., Bahmani Z., Moradi B., Bay A., Pouya R.H.; Metal concentrations in fillet and gill of parrotfish (Scarus ghobban) from the Persian Gulf and implications for human health, Food Chem. Toxicol., 118, 348–354 (2018).
5. Miri M., Akbari E., Amrane A., Jafari S.J., Eslami H., Hoseinzadeh E., Zarrabi M., Salimi J., Sayyad-Arbabi M., Taghavi M.; Health risk assessment of heavy metal intake due to fish consumption in the Sistan region, Iran. Environ. Monit. Assess., 189, 583-593 (2017).
6. Bhatia R., Singh R.; A review on nanotechnological application of magnetic iron oxides for heavy metal removal, J. Water Process Eng., 31, 100845-100855 (2019).
7. Yang J., Hou B., Wang J.; Nanomaterials for the removal of heavy metals from wastewater, Nanomaterials, 9, 424-462 (2019).
8. Kamnoet P., Aeungmaitrepirom W., Menger R.F., Henry C.S.; Highly selective simultaneous determination of Cu(II), Co(II), Ni(II), Hg(II), and Mn(II) in water samples using microfluidic paper-based analytical devices, Analyst , 146, 2229–2239 (2021).
9. Fouda-Mbanga B.G., Prabakaran E., Pillay K.; Carbohydrate biopolymers, lignin based adsorbents for removal of heavy metals (Cd^{2+}, Pb^{2+}, Zn^{2+}) from wastewater, regeneration and reuse for spent adsorbents including latent fingerprint detection, Biotechnology Reports, 30, 1-16 (2021).
10. Farhan M.A., Dheyab H.B., Hasan A.A.; Synthesis and Characterization of cellulose grafted maleic anhydride and substituted it with Amoxicillin, European J. Of Pharmaceutical and medical research, 12, 84-90 (2017).
11. Gurdag G., Sarmad S.; Cellulose Graft Copolymers: Synthesis, Properties and Applications, Polysaccharide Based Graft Copolymers, 15-57 (2013).
12. Wojna´rovits L., Fo¨ldva´ry C.M., Taka´cs E.; Radiation-induced grafting of cellulose for adsorption of hazardous water pollutants: a review, Radiat. Phys. Chem., 79, 848–862 (2010).
13. Ngwuluka C.N., Ochekpe A.N., Aruoma I.O.; Naturapolyceutics: The Science of Utilizing Natural Polymers for Drug Delivery, Polymers, 6, 1312-1332 (2014).
14. Dakiky M., Khamis M., Manassra A., Mer'eb M.; Selective adsorption of chromium (VI) in industrial wastewater using low-cost abundantly available adsorbents, J. Adv. Environ. Res., 6, 533- 540 (2002).
15. Dinu M.V., Dragan E.S.; Heavy metals adsorption on some iminodiacetate chelating resins as a function of the adsorption parameters, React. Funct. Polym., 68, 1346 -1354 (2008).
16. Dinu M.V., Dragan E.S., Trochimczuk A.W.; Sorption of Pb(II) Cd(II) and Zn(II) by iminodiacetate chelating resins in non-competitive and competitive conditions, Desalination, 249, 374-379 (2009).
17. Elmorsi T.M.; Equilibrium isotherms and kinetic studies of removal of methylene blue dye by adsorption onto miswak leaves as a natural adsorbent, Journal of Environmental Protection, 2, 8-17 (2011).
18. El-Qada E.N., Allen S.J., Walker G.M.; Adsorption of methylene blue onto activated carbon produced from steam activated bituminous coal a study of equilibrium adsorption isotherm, J. Chem. Eng., 124, 103-110 (2006).
19. Garg U.K., Kaur M.P., Garg V.K., Sud D.; Removal of Hexavalent Chromium from Aqueous Solution by Agricultural Waste Biomass, J. Hazard Mater., 1, 40-60 (2007).

20. Gupta S.S., Bhattacharyya K.G.; Immobilization of Pb(II) Cd(II) and Ni(II) ions on kaolinite and montmorillonite surfaces from aqueous medium, J. of Environmental Management, 8, 7-46 (2008).
21. Abouzayed F.I., Abo El-nassr N.T., Abouel-Enein S.A.; Synthesis, Characterization of functionalized grafted cellulose and its environmental application in uptake of copper(II),manganese(II) and iron(III) ions, Journal of Molecular Structure, 1270, 133907 (2022).
22. Pulat M., Isakoca C.; Chemically induced graft copolymerization of vinyl monomers onto cotton fibers, J. Appl. Polym. Sci., 100, 2343–2347 (2006).
23. Edson C.S.F., Luciano C.B. L., Fabrícia C.S., Kaline S.S., Maria G.F., Sirlane A.A.S.; Immobilization of ethylene sulfide in aminated cellulose for removal of the divalent cations, J. Carbohydrate Polymers, 92, 1203–1210 (2013).
24. Liu L., Pan Y., Bhushan B., Zhao X.; Mechanochemical robust, magnetic-driven, superhydrophobic 3D porous materials for contaminated oil recovery, J. Colloid Inter. Sci., 538, 25–33 (2019).
25. Liu S., Sun G.; Radical graft functional modification of cellulose with allyl monomers: Chemistry and structure characterization, Carbohyd. Polym., 71, 614–625 (2008).
26. Monier M., El-Sokkary A.M.A.; Modification and characterization of cellulosic cotton fibers for efficient immobilization of urease, Int. J. Biol. Macromol., 51, 18–24 (2012).
27. Dacrory S., Abou-Yousef H., Kamel S., Abou-zeid R.E., Abdel- Aziz M.S., ELbadry M.; Functionalization and cross linking of carboxymethyl cellulose in aqueous media, Cellulose Chem. Technol., 53, 23-33 (2019).
28. El-Aarag B., Fathy A.E., Salem T., Khedr N., Khalifa S.A.M., El-Seedi H.R.; New metal complexes derived from diacetylmonoxime-n(4) antipyrinylthiosemicarbazone: Synthesis, characterization and evaluation of antitumor activity against Ehrlich solid tumors induced in mice, Arabian Journal of Chemistry, 14, 1-16 (2021).
29. Fu F., Ma J., Xie L.; Chromium removal using resin supported nanoscale zero-valent iron, J. Environ. Manag., 128, 822-827 (2013).
30. Wadhawan S., Jain A., Nayyar J., Mehta S.K.; Role of nanomaterials as adsorbents in heavy metal ion removal from waste water: a review, J. Water Process Eng., 33, 101038-101054 (2020)
31. Sen T.K., Gomez D.; Adsorption of zinc (Zn^{+2}) from aqueous solution on natural bentonite, Desalination, 267, 286-294 (2011).
32. Aljeboree A.M., Alshirif A.N., Alkaim A.F.; Kinetics and Equilibrium Study for the Adsorption of Textile Dyes on Coconut Shell activated carbon, Arabian. J. Chemistry, 10, 3381-3393 (2017).
33. Igberase E., Osifo P., Ofomaja A.; The adsorption of Pb, Zn, Cu, Ni, and Cd by modified ligand in a single component aqueous solution: equilibrium, kinetic, thermodynamic, and desorption studies, International Journal of Analytical Chemistry, 2017, 1-15 (2017).
34. Malkoc E., Nuhoglu Y., Dundar M.; Adsorption of chromium (VI) on pomace-an olive oil industry waste: batch and column studies, Journal of Hazardous Materials, 138, 142-151 (2006).
35. Singh S., Kapoor D., Khasnabis S., Singh J., Ramamurthy P.C.; Mechanism and kinetics of adsorption and removal of heavy metals from wastewater using nanomaterials, Environmental Chemistry Letters, 19, 2351–2381 (2021).
36. Dubey R., Bajpai J., Bajpai A.K.; Chitosan-alginate nanoparticles (CANPs) as potential nanosorbent for removal of Hg (II) ions, Environ. Nanotechnol. Monit. Manag., 6, 32–44 (2016).
37. Silva S.P., Sousa S., Rodrigues J.; Adsorption of Acid Orange 7 Dye in Aqueous Solutions by Spent Brewery Grains, J. Sep. Purif. Technol., 40, 309–315 (2004).
38. Qiu H., Lv L., Pan B.C., Zhang Q.J., Zhang M.; Critical review in adsorption kinetic models, J. Zhejiang University Science A., 10, 7-16 (2009).
39. El Qada E.N., Allen S.J., Walker G.M.; Adsorption of methylene blue onto activated carbon produced from steam activated bituminous coal: a study of equilibrium adsorption isotherm, Chemical Engineering Journal, 124, 103–110 (2006).
40. Ghoniem M.M., El-Desoky H.S., El-Moselhy K.M., Amer A., AboEl-Naga E.H., Mohamedein

L.I., Al-Prol A. E.; Removal of cadmium from aqueous solution using green marine algae, Ulva lactuca, Egypt. J. Aquat. Res., 40, 235–242 (2014).

41. Abouel-Enein S.A., Okbah M.A. , Hussain S.G. , Soliman N.F., Ghounam H.H.; Adsorption of Selected Metals Ions in Solution Using Nano-Bentonite Particles: Isotherms and Kinetics, Environmental Processes, 7, 463-477 (2020).
42. Shama S.A., Gad M.A.; Removal of heavy metals (Fe^{3+}, Cu^{2+}, Zn^{2+}, Pb^{2+}, Cr^{3+} and Cd^{2+}) from aqueous solutions by using hebba clay and activated carbon, Port. Electrochim. Acta., 28, 231–239 (2010).
43. Asif Z., Chen Z.; Removal of arsenic from drinking water using rice husk, Journal of Applied Water Science, 7, 1449-1458 (2017).
44. Fathy A.E., Abouel-Enein S.A., El-shinawy F.; Removal of Lead and Copper Ions from Polluted Aqueous Solutions using Nano-Sawdust Particles, International journal of waste resources, 7, 1000305-1000311 (2017).
45. Ragab E.A., Kholod H.K., Abd El-Aziz M.E., Morsi S.M., Samir K.; Grafted TEMPO-oxidized cellulose nanofiber embedded with modified magnetite for effective adsorption of lead ions, International Journal of Biological Macromolecules, 167, 1091-1101 (2018).
46. Kumar R., Sharma R.K., Singh A.P., Removal of organic dyes and metal ions by cross-linked graft copolymers of cellulose obtained from the agricultural residue, Journal of Environmental Chemical Engineering, 6, 6037-6048 (2018).
47. Kumar R., Sharma R.K., Singh A.P.; Synthesis and characterization of cellulose based graft copolymers with binary vinyl monomers for efficient removal of cationic dyes and Pb(II) ions, Journal of Polymer Research, 135, 1-20 (2019).
48. Hizkeal T.K., Sisay T.N., Fedlu K.S.; Adsorptive Removal of Cd(II) Ions from Wastewater Using Maleic Anhydride Nanocellulose, Journal of Nanotechnology, 2021, 1-15 (2021).
49. Hong T.T., Okabe H., Hidaka Y., Hara K. ; Removal of metal ions from aqueous solutions using carboxymethyl cellulose/sodium styrene sulfonate gels prepared by radiation grafting, Carbohydrate Polymers, 157, 335-343 (2017).
50. Gamze G., Gulten G., Saadet O.; Competitive Removal of Heavy Metal Ions by Cellulose Graft Copolymers, Journal of Applied Polymer, 90, 2034-2039 (2003).